

Predicting boiling heat transfer using computational fluid dynamics

J G Hawley*, M Wilson, N A F Campbell, G P Hammond and M J Leathard

Department of Mechanical Engineering, Faculty of Engineering and Design, University of Bath, UK

Abstract: A study has been undertaken to assess the capability of incorporating different empirical approaches in a computational fluid dynamics (CFD) environment for predicting boiling heat transfer. The application is for internal combustion (IC) engine cooling galleries and experimental validation work has been undertaken. Three different boiling heat transfer models are described, one based on the principle of superposition (Chen) and two based on the partial boiling method (Thom and Cipolla). Overall, the Thom partial boiling approach was found to be the most representative of the three considered. However, numerous issues were found to be evident whatever approach was adopted and these are discussed in the paper. The partial boiling model was found to be the most simple to incorporate in the CFD model.

Keywords: boiling heat transfer, CFD, IC engines

NOTATION

c_p	specific heat capacity (J/kg K)
CFD	computational fluid dynamics
F	Chen Reynolds number factor
h	heat transfer coefficient (W/m ² K)
l_v	specific latent heat of vaporization (J/kg)
k	thermal conductivity (W/m K)
Nu	Nusselt number
ONB	onset of nucleate boiling
p, P	pressure (N/m ²)
Pr	Prandtl number
q''	heat flux (W/m ²)
Re	Reynolds number
S	Chen suppression factor
T	temperature (°C)
μ	dynamic viscosity (kg/m s)
ρ	density (kg/m ³)
σ	surface tension (N/m)

Subscripts

boil	boiling
conv	convective
l	liquid

mac	macro-convective
mic	micro-convective
nuc	nucleate boiling
onb	onset of nucleate boiling
sat	saturation
tp	two phase
v	vapour
w	property value at the wall temperature
∞	bulk value

1 INTRODUCTION

Computational fluid dynamics (CFD) is used for the prediction of the heat transfer coefficient associated with the coolant flows at the metal/liquid interface of cooling galleries within internal combustion engines. A 'wall function' is often used to determine the heat transfer coefficient based on local velocity and fluid properties. The heat transfer coefficient derived from this is subsequently used as a boundary condition within finite element (FE) analysis to predict component metal temperatures. Subsequently, the temperatures of specific areas of the engine can be determined to assess likely integrity and durability issues. This is undertaken under conditions of forced convective heat transfer, as current engine design does not allow for excursions into the nucleate boiling regime [1].

Boiling is an extremely advantageous mechanism, due to the ability to extract higher rates of heat transfer for

The MS was received on 21 May 2003 and was accepted after revision for publication on 21 January 2004.

** Corresponding author: Department of Mechanical Engineering, Faculty of Engineering and Design, University of Bath, Bath BA2 7AY, UK.*

only small increases in surface temperatures. However, this two-phase heat transfer mechanism has only been considered superficially for the internal combustion engine application, mainly due to the inherent risks associated with the intentional generation of vapour. Generated vapour can lead to two potentially undesirable situations:

1. **Blockage.** Cylinder heads usually contain small diameter passages, which are used to provide coolant to target specific areas. The generation of bubbles could lead to the blocking of such passages, thereby restricting at times the incoming coolant flow. Although this condition is undesirable, it is not as damaging as the production of vapour blankets.
2. **Vapour blankets.** At extremely high heat fluxes the bubble activity at the heated surface can become so intense that a vapour blanket forms. This is observed in Fig. 1, which shows a photograph taken of this condition on the thermal flow rig used for these investigations (Fig. 2). At the heated section coolant interface, the heat flux level has become so high that the vapour blanket on the leading edge can be clearly seen. Under such conditions, the blanket of vapour bubbles acts as an insulator preventing heat from

escaping. Subsequently, if this condition were experienced in an engine, it would quickly overheat and suffer catastrophic failure. This vapour blanket condition is usually referred to as 'film boiling'. For film boiling to exist, a critical heat flux (CHF) level must have been exceeded.

Flow boiling, with its enhanced heat transfer rates, may result in one or a number of desirable features, which include reduced coolant flows, faster engine warm-up and higher engine operating temperatures, in turn resulting in some benefits with regard to emissions and fuel consumption. However, the scientific aspects of flow boiling heat transfer in small irregular passages are not well understood and any boiling-based strategy requires promotion and control. A purely theoretical approach has yet to be realized and CFD in this area is still largely concerned with fundamental research into modelling of the boiling process.

The majority of predictive work undertaken on flow boiling has been empirical in approach. The work reported here has attempted to utilize this empirical work by incorporating certain empirical models into a CFD environment. Three models have been selected for evaluation:



Fig. 1 Section of the heated testpiece at the metal/coolant interface. Front portion of the heated sample is covered by a vapour film blanket. The CHF has been achieved

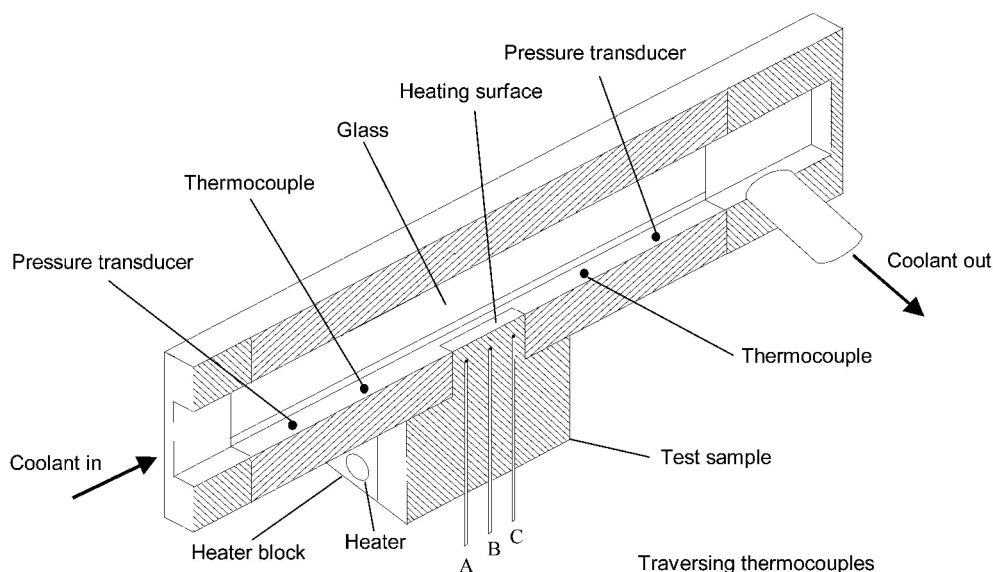


Fig. 2 Simulated engine cooling gallery [6]

1. Chen [2]. A large proportion of published work has considered the Chen correlation for the internal combustion (IC) engine application.
2. Thom *et al.* [3]. This approach is based on partial boiling and is attractive for inclusion into the CFD environment as the heat transfer predictions are based on local fluid pressures and properties. These are readily available within each solution cell of the CFD model.
3. Cipolla [4]. This is based on the Thom model, but developed using data under conditions found in IC engine cooling galleries.

In this work, these three models have been incorporated into a CFD package to provide predictions of heat transfer coefficients validated against experimental results from a thermal flow rig. The rig was specifically designed to replicate, as far as possible, the thermofluid situations that are found in IC engine cooling galleries and it has formed the basis of numerous heat transfer studies undertaken and reported by researchers at Bath [5]. The overall aim of the work reported here is to develop a suitable and robust technique for the prediction of boiling heat transfer in IC engine cooling galleries using CFD. This is considered a desirable feature within the design process for future engine development.

2 HEAT TRANSFER

A brief summary of the methods used in this study to model boiling heat transfer is given. However, a short description of the test rig is first provided, as its features directly affect the method of determining convective heat transfer data.

A simulated engine-cooling gallery, shown in Fig. 2, was used to generate experimental data to validate the CFD approach. The rig was designed, as far as possible, to replicate the thermofluid, physical and material conditions that would be expected within an IC engine-cooling gallery [6]. A typical antifreeze solution is used and the heat transfer coefficients are inferred at the surface of the heat-conducting testpiece via traversing thermocouples. The testpiece is aluminium with an as-cast surface finish.

The three models chosen for inclusion in the CFD package can be considered to follow the principle of superposition or adopt the partial boiling approach.

2.1 Principle of superposition

Nucleate boiling heat transfer can be superimposed on to forced convection heat transfer. This is known as the principle of superposition. Collier and Thome [7] suggest the following algorithm to determine the heat transfer

under conditions of subcooled boiling:

$$q'' = h_{\text{mac}}(T_w - T_\infty) + h_{\text{mic}}(T_w - T_{\text{sat}}) \quad (1)$$

2.1.1 Convective approach

The convective component has previously adopted the very widely used Dittus–Boelter equation for fully developed, turbulent flow in pipes. This gives the Nusselt number (Nu) (a non-dimensionalized form of the heat transfer coefficient) as the product of the Reynolds number (Re) and Prandtl number (Pr) effects:

$$Nu = 0.023Re^{0.8}Pr^{0.4} \quad (\text{for } T_\infty < T_w) \quad (2)$$

In an extensive study to determine representative IC engine convective heat transfer data from the thermal flow rig also used for this work, the Dittus–Boelter correlation has been modified to fulfil the following requirements [6]:

1. The hydrodynamic entry length. The flow is not fully developed over the heated sample. The Dittus–Boelter correlation applies to flow that is fully developed, both hydrodynamically and thermally.
2. The unheated starting length. Heat transfer does not begin at the duct entrance, but at a distance downstream. The Dittus–Boelter correlation applies to flow where the thermal and velocity boundary layers begin to develop simultaneously.
3. The rough surface of the heated sample. The Dittus–Boelter correlation applies strictly to hydraulically smooth ducts.
4. The sensitivity of fluid physical properties to temperature. The Dittus–Boelter correlation assumes that fluid properties are adequately represented by their value at the film temperature.

Combining these four factors with the Dittus–Boelter expression leads to a modified expression, as reported previously by Robinson *et al.* [8]:

$$Nu = (\text{Dittus–Boelter correlation}) \times (\text{entrance factor}) \\ \times (\text{unheated starting length factor}) \\ \times (\text{roughness factor}) \times (\text{viscosity loading factor}) \quad (3)$$

2.1.2 Boiling approach

Chen [2] suggested the following equation to determine the micro, or boiling, heat transfer coefficient:

$$h_{\text{mic}} = 0.00122 \left(\frac{k_l^{0.79} (C_p)_l^{0.45} \rho_l^{0.49}}{\sigma^{0.5} \mu_l^{0.29} h_{lv}^{0.24} \rho_v^{0.24}} \right) \Delta T_{\text{sat}}^{0.24} \Delta P_{\text{sat}}^{0.75} (S) \quad (4)$$

The subscripts l and v refer to the liquid and vapour phases. ΔT_{sat} is the difference between the wall temperature and the saturation temperature. The difference

between the wall pressure and the saturation pressure ($P_w - P_{sat}$) is ΔP_{sat} .

A set of algorithms given by Kreith and Bohn [9] and used by Gollin *et al.* [10] can be used to determine the suppression factor, S , given graphically by Chen [2]. These algorithms are based on the two-phase Reynolds number, Re_{tp} . For values of $Re_{tp} < 32.5$,

$$S = \frac{1}{1 + 0.12Re_{tp}^{1.14}} \quad (5)$$

where

$$Re_{tp} = Re F^{1.25} \times 1 \times 10^{-4}$$

For subcooled flow boiling heat transfer, F is equal to one.

2.2 Partial boiling method

Figure 3 shows the principle used to model boiling heat transfer, known as the partial boiling method. This method defines three regions in the heat transfer process. The first is the single-phase forced convection region. At a temperature slightly above the saturation temperature, boiling will start, initially at a small number of locations on the surface. This point is known as the onset of nucleate boiling (ONB) point and occurs at a temperature T_{onb} .

The temperature T_{onb} is calculated using the following [11], where the heat flux at the ONB point, q''_{onb} , can be calculated from the single-phase forced convection heat transfer:

$$T_{onb} - T_{sat} = \left(\frac{8\sigma q''_{onb} T_{sat}}{h_{lv} k_1 \rho_v} \right)^{1/2} \quad (6)$$

At higher surface temperatures, boiling becomes more developed across the entire surface and dominates the

heat transfer process. This is known as the fully developed boiling region. In this region, the coolant velocity and the inlet subcooling have little effect on the boiling heat transfer [7]. This region has been modelled using two equations developed by Thom *et al.* [3] and Cipolla [4].

2.2.1 Thom *et al.* (1965) [3]

Thom *et al.* studied nucleate subcooled boiling of water using a heated tubular test section. From this, an equation relating ΔT_{sat} , flux and pressure was proposed:

$$q'' = \left(\frac{\Delta T_{sat}}{22.65 e^{-(p/87 \times 10^5)}} \right)^2 \times 10^6 \quad (7)$$

2.2.2 Cipolla (1989) [4]

Cipolla's correlation development was based on the Thom *et al.* algorithm. However, Cipolla states that an 'anti-freeze mixture' rather than water was used, but does not give any further details:

$$q'' = 0.73 \times 10^4 e^{2.33 \times 10^{-6} P} \Delta T_{sat}^{1.27} \quad (8)$$

Cipolla shows some success with matching experimental data with these algorithms at different velocities, although the scatter on the data is significant.

The region between the forced convection and the fully developed boiling is known as the partial boiling region. In this region, after the onset of nucleate boiling, the forced convection and fully developed boiling curves are interpolated, as given by [12]

$$q'' = q''_{conv} \left\{ 1 + \left[\frac{q''_{boil}}{q''_{conv}} \left(1 - \frac{q''_B}{q''_{boil}} \right) \right]^2 \right\}^{1/2} \quad (9)$$

Equation (7) or (8) is used to calculate q''_{boil} and q''_B , where q''_B is calculated by substituting $T_{onb} - T_{sat}$ for ΔT_{sat} .

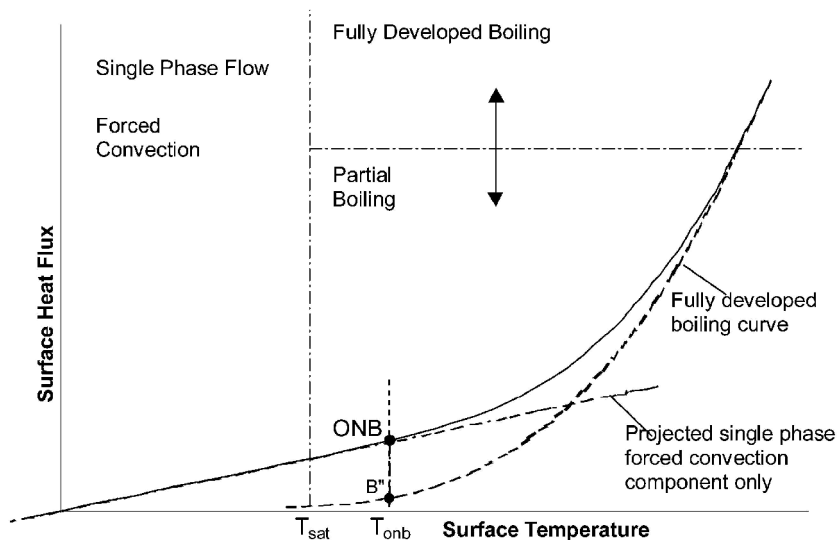


Fig. 3 Partial boiling method

The use of the onset of nucleate boiling point, T_{onb} , to delay boiling until the wall temperature is above the saturation temperature can be seen as a form of boiling suppression. Bjorge *et al.* [13] state that the term multiplying the q''_{boil} term in equation (9) is effectively Chen's boiling suppression factor. However, once the fully developed boiling region has been reached, boiling dominates and it is convection that is suppressed.

3 METHODOLOGY

The simulated engine-cooling gallery studied experimentally was modelled using the (finite volume) computational fluid dynamics (CFD) package STAR-CD. Figure 4 shows the geometry of the three-dimensional CFD model. Steady-flow computations were carried out using the high Reynolds number $k-\epsilon$ turbulence model,

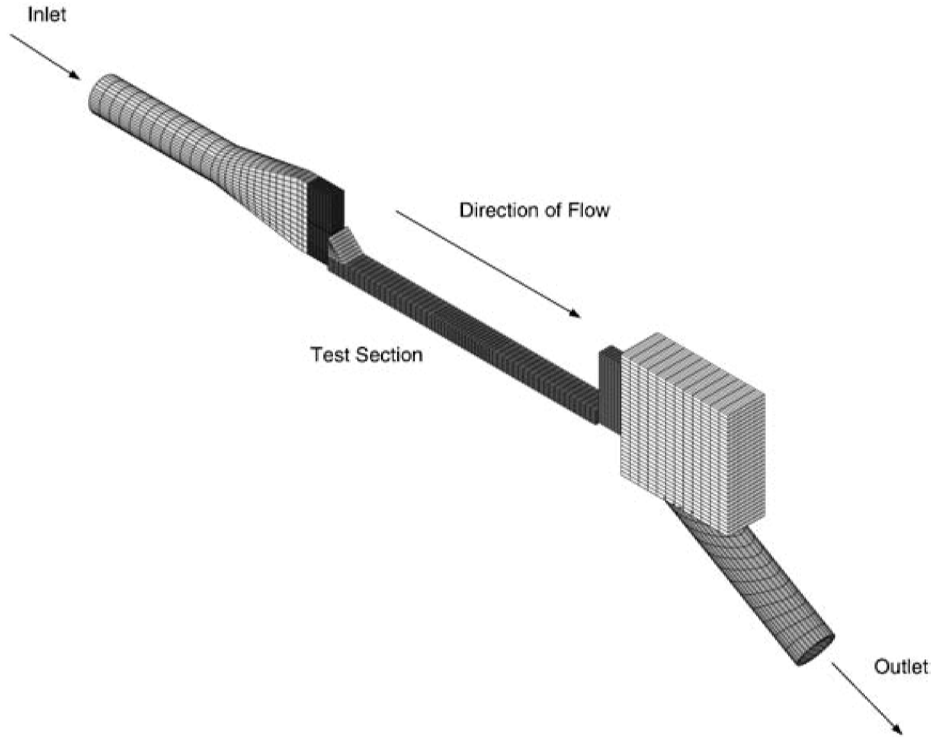


Fig. 4 CFD model of simulated engine cooling gallery [16]

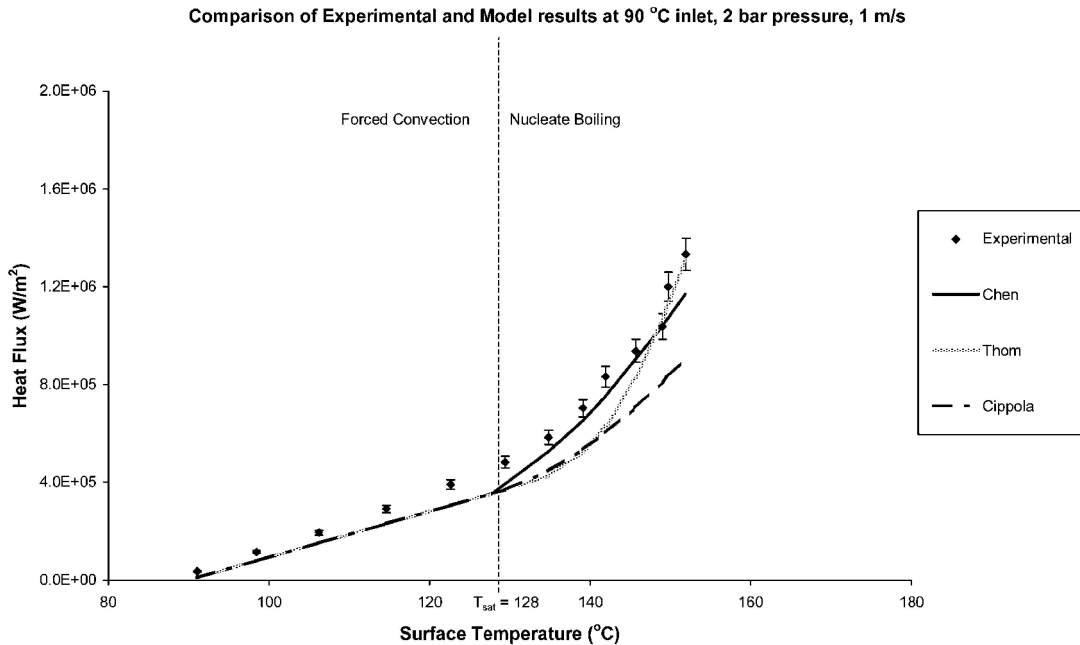


Fig. 5 Boiling model comparisons

with wall functions used to describe the near-wall flow. A 10×12 (vertical \times horizontal) mesh was used in the duct test section, with 18 planes spanning the heated testpiece in the downstream direction. Sensitivity tests were carried out to confirm that computed heat transfer results were not affected by the mesh spacing at this level of resolution or by the assumed inlet conditions. The computed flow provides the velocity, temperature and pressure information required by the different boiling models.

The nucleate boiling heat transfer models described above were implemented through the user coding interface to the CFD package, in order to calculate

wall surface heat transfer coefficients that then affect the computed fluid temperatures. The computed fluid dynamics is not affected; no attempt is made to model bubble generation or the movement of bubbles in the fluid. This pragmatic approach to the modelling is a development of existing techniques, which gives rise to a practical implementation requiring only modest computing resources. This can be compared with the resources required for detailed modelling of even a single bubble site (see Son *et al.* [14]).

Some of the heat transfer models rely upon global parameters, such as duct diameter, and these are not available directly within the CFD mesh-cell-based

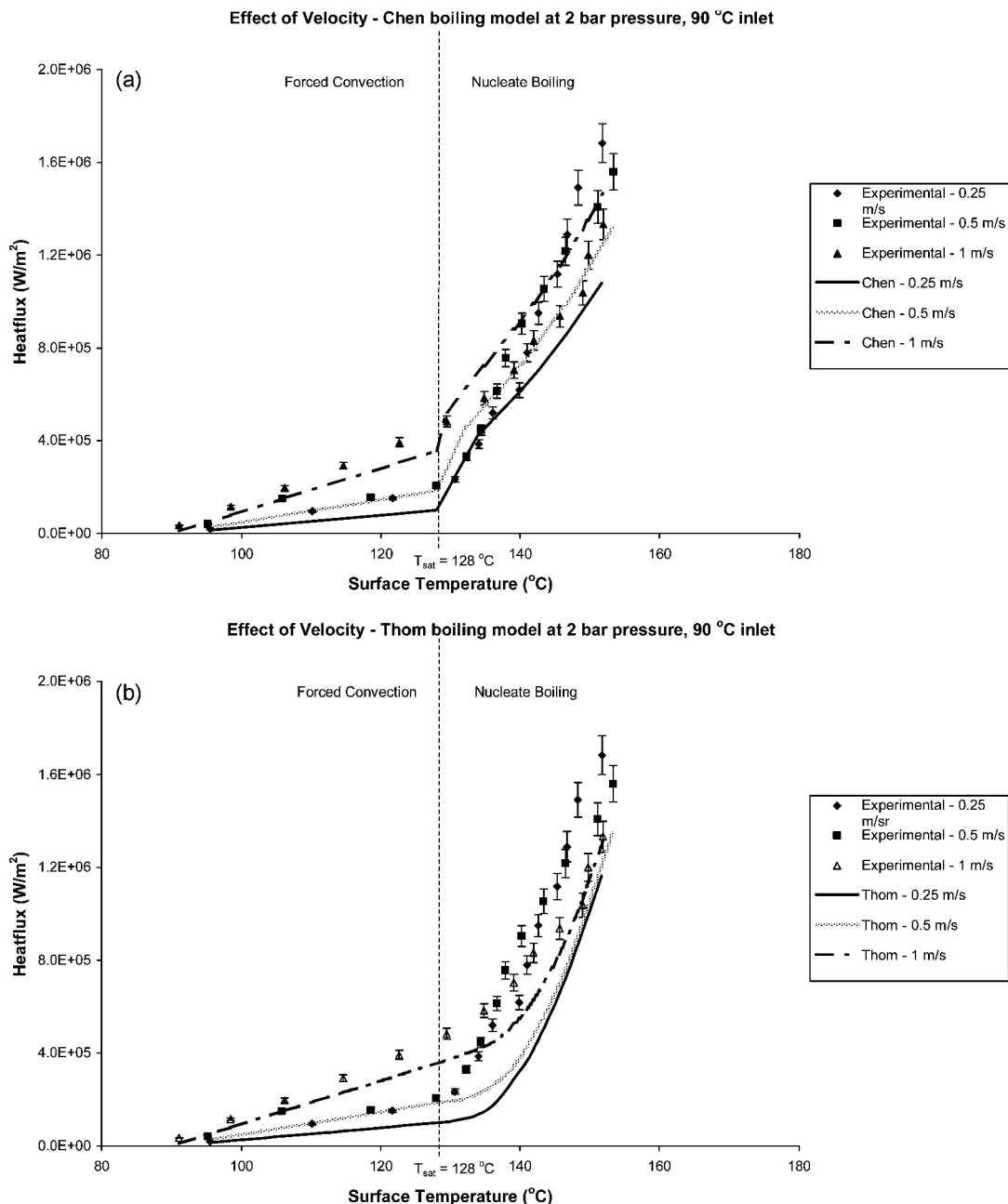


Fig. 6 (continued over)

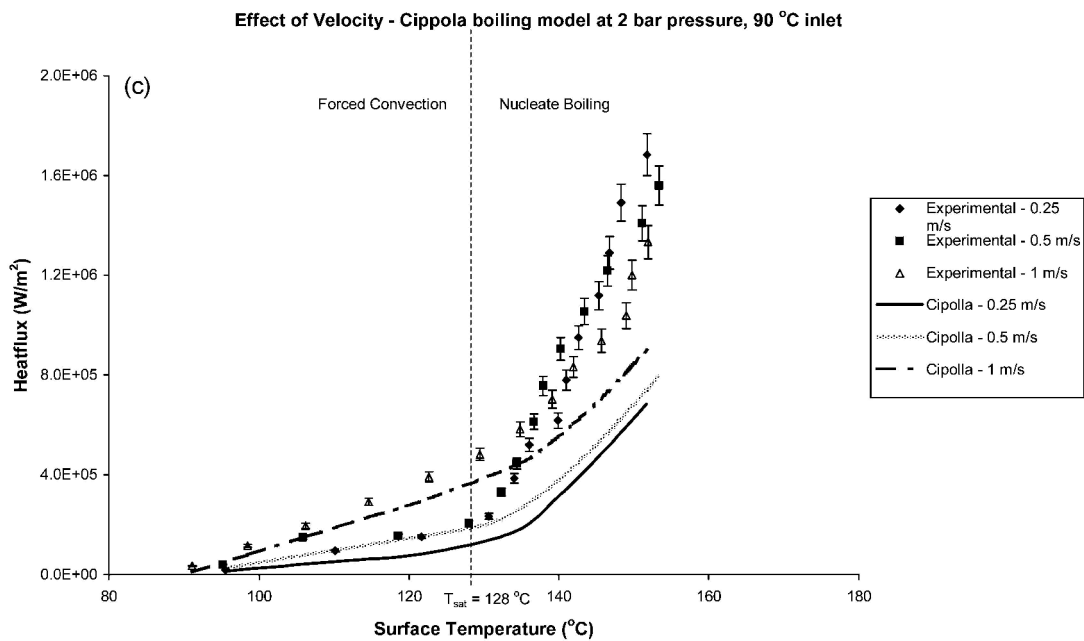


Fig. 6 Effect of velocity: (a) Chen boiling mode, (b) Thom boiling model and (c) Cipolla boiling model

solution procedure. For this initial implementation, these parameters were provided explicitly where necessary as part of the user coding. For the Chen model, the two-phase Reynolds number is based on the velocity in the cell and the duct diameter. All of the fluid properties, temperatures and pressures are taken from individual cell values. The Cipolla and Thom models make use of only local pressure and temperature values, making the CFD implementation straightforward.

4 RESULTS

Figure 5 shows results for the three different boiling models in comparison with measured data for a standard default test. The bars on the experimental data indicate the estimated uncertainty in the results, as described by Robinson [6]. In the forced convection regime, i.e. for $T < T_{\text{sat}}$, the results given by the composite convection model of Robinson are superior to those produced by the 'standard' wall function for heat transfer [15]. This is due to the developing nature of the (hydrodynamic and thermal) boundary flow in the duct at the heated test piece location [16]. This also influences the performance of the models in the nucleate boiling region, as a result of accounting for the combined effects of convection and boiling.

Figure 5 shows that, in the nucleate boiling regime, the Cipolla model underpredicts the experimental results, while the Thom model gives improved agreement with the measurements at higher values of surface temperature (and hence higher heat flux). The Chen model gives a prediction in reasonable agreement with the

measurements throughout the nucleate boiling region over the range studied.

The performance of the three boiling models, and the computed and measured parametric effects of the cooling flow velocity, system pressure and fluid temperature on heat transfer, are described below.

4.1 Effect of bulk velocity on heat transfer

The effect of varying the bulk cooling flow velocity on the computed and measured heat transfer is shown in Figs 6a to c for the Chen, Thom and Cipolla models respectively. For each model, increased velocity leads to increased heat transfer in both the forced convection and nucleate boiling regions. The Chen model (Fig 6a) appears to reproduce the measured variations well. The computed rapid increase in heat transfer at the saturation temperature, above which boiling begins, is a result of the superposition of convection and boiling effects used by this model.

In the boiling region, the measurements converge (within the limits of experimental uncertainty), suggesting that changes in velocity are less significant than in the convection region. This effect has been shown by a number of workers, including Bergles and Rohsenow [12]. Only the Thom model (Fig. 6b) shows similar behaviour to this measured trend, although the level of heat transfer is underpredicted compared with the experimental results. The use of the onset of nucleate boiling (ONB) point, in the partial boiling method used by the Thom and Cipolla models, appears to give a better representation of the gradual measured increase in heat flux for surface temperatures above the saturation

temperature, compared with the Chen model. The Cipolla model (Fig. 6c), however, significantly underpredicts the measurements in the boiling region.

4.2 Effect of pressure variation

Changing the system pressure changes the fluid saturation temperature, the temperature at which boiling can be initiated. This relationship is shown in Table 1 for system pressures of 1, 2 and 3 bar, and computed and measured heat transfer results for these conditions are described below.

Table 1 Saturation temperature variation

Absolute pressure (bar)	Saturation temperature (°C)
1	108
2	128
3	142

Figures 7a to c show the effect of pressure on the computed and measured variation of heat flux with surface temperature. Figure 7a shows that the Chen model gives the same general trend as the experimental results;

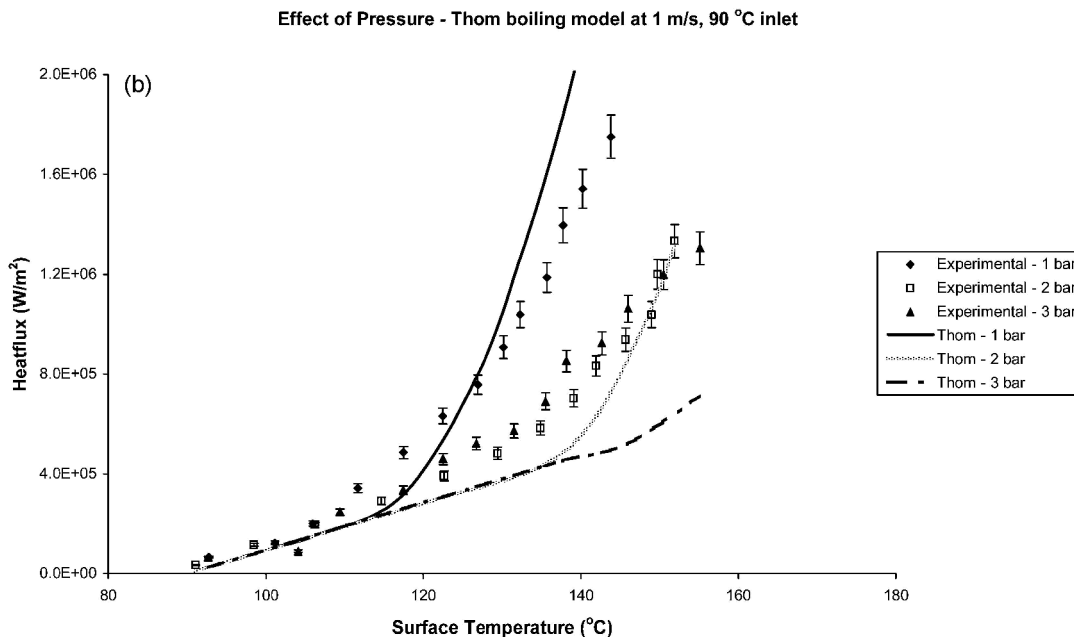
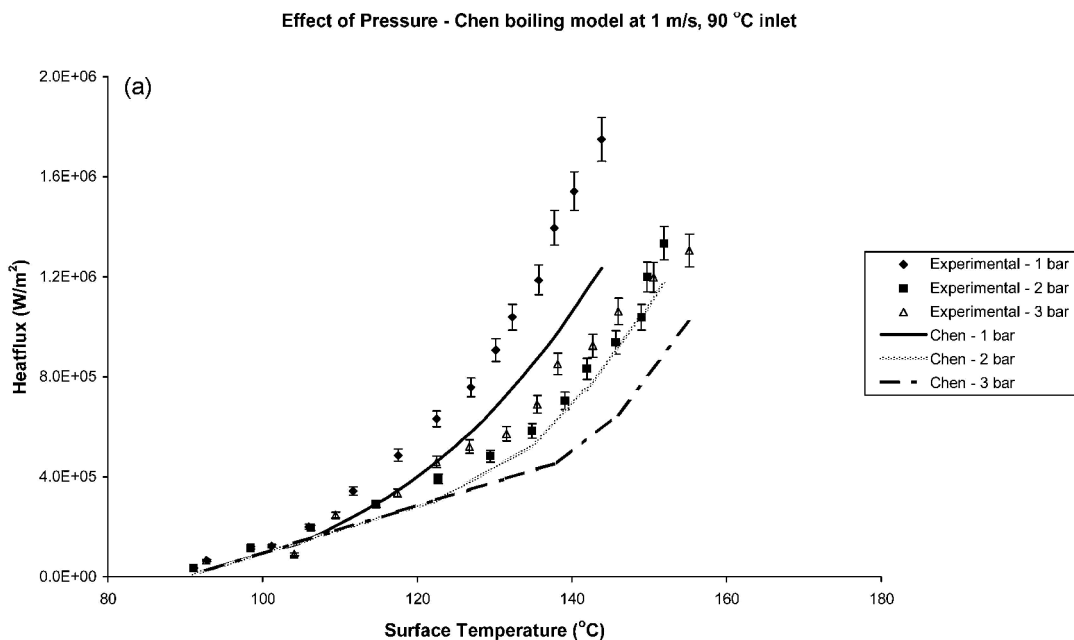


Fig. 7 (continued over)

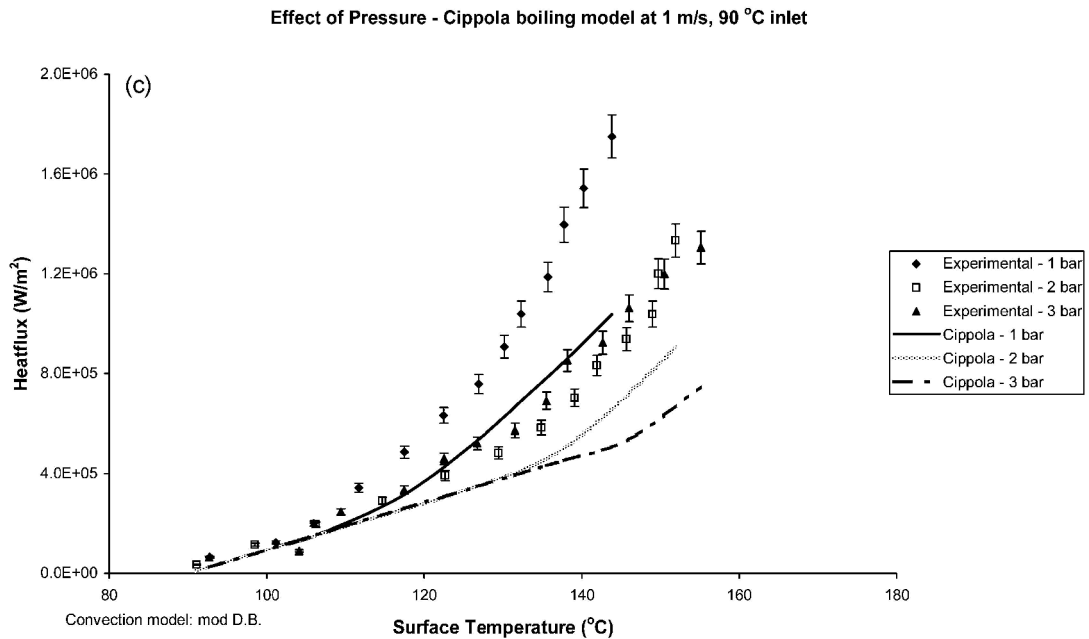


Fig. 7 Effect of pressure: (a) Chen boiling model, (b) Thom boiling model and (c) Cippola boiling model

a reduced system pressure results in increased heat transfer provided that boiling is taking place. The measured results at 2 bar system pressure are reproduced reasonably well; the measured results at 1 and 3 bar are underpredicted. The predictions given by the Thom model show reasonable trends (Fig. 7b) although some of the 1 bar measurements are overpredicted. The Cippola model (Fig. 7c) generally underpredicts the measurements.

4.3 Effect of fluid temperature variation

Figures 8a to c show the computed effect of fluid temperature variation on heat transfer coefficients for each of the three models, in comparison with experimental results for fluid temperatures of 60, 90 and 120 °C. For the Chen model (Fig. 8a), there is little effect of the fluid temperature on the predicted heat transfer coefficients. The measurements, however, show a much larger variation. The Thom and Cippola model results (Figs 8b and c respectively) both show a more significant effect of fluid temperature than the Chen model. For the highest fluid temperature, the Cippola boiling model appears to show a similar trend to the experimental results in tending towards a constant value as the wall surface temperature increases.

4.4 Overall accuracy

To determine the accuracy of each model in predicting the experimental results, a method is required to define the difference between the experimental and predicted results. Wambsganss *et al.* [17] define a mean deviation

for comparing predicted and experimental results. This mean deviation is given in the following equation and is used by Campbell [18] to consider the accuracy of heat transfer correlations:

$$\text{Mean deviation} = \frac{1}{N} \sum \frac{|q_{\text{pred}} - q_{\text{exp}}|}{q_{\text{exp}}} \times 100\% \quad (10)$$

Overall, the Thom model was found to predict the set of experimental results shown in Table 2, with the minimum difference at an overall mean deviation of 36.4 per cent. The Chen model is close behind at 40.6 per cent and the Cippola model at 41.2 per cent is very close to the Chen model. It should be noted that some sets of experimental data can be significantly underpredicted (e.g. data at 120 °C inlet temperature, Table 2 and Figs 8a to c).

5 CONCLUSIONS

Three boiling heat transfer models have been incorporated into a computational fluid dynamics model. The results have been compared with experimental results from a simulated engine-cooling gallery bench rig.

Overall, the Thom model was found to predict the experimental results with the minimum difference, with a mean deviation of 36.4 per cent, followed closely by the Chen model at 40.6 per cent. In general, the Chen model represents parametric variations well, except at certain conditions such as changes in the bulk fluid temperature. It is also problematic to incorporate into

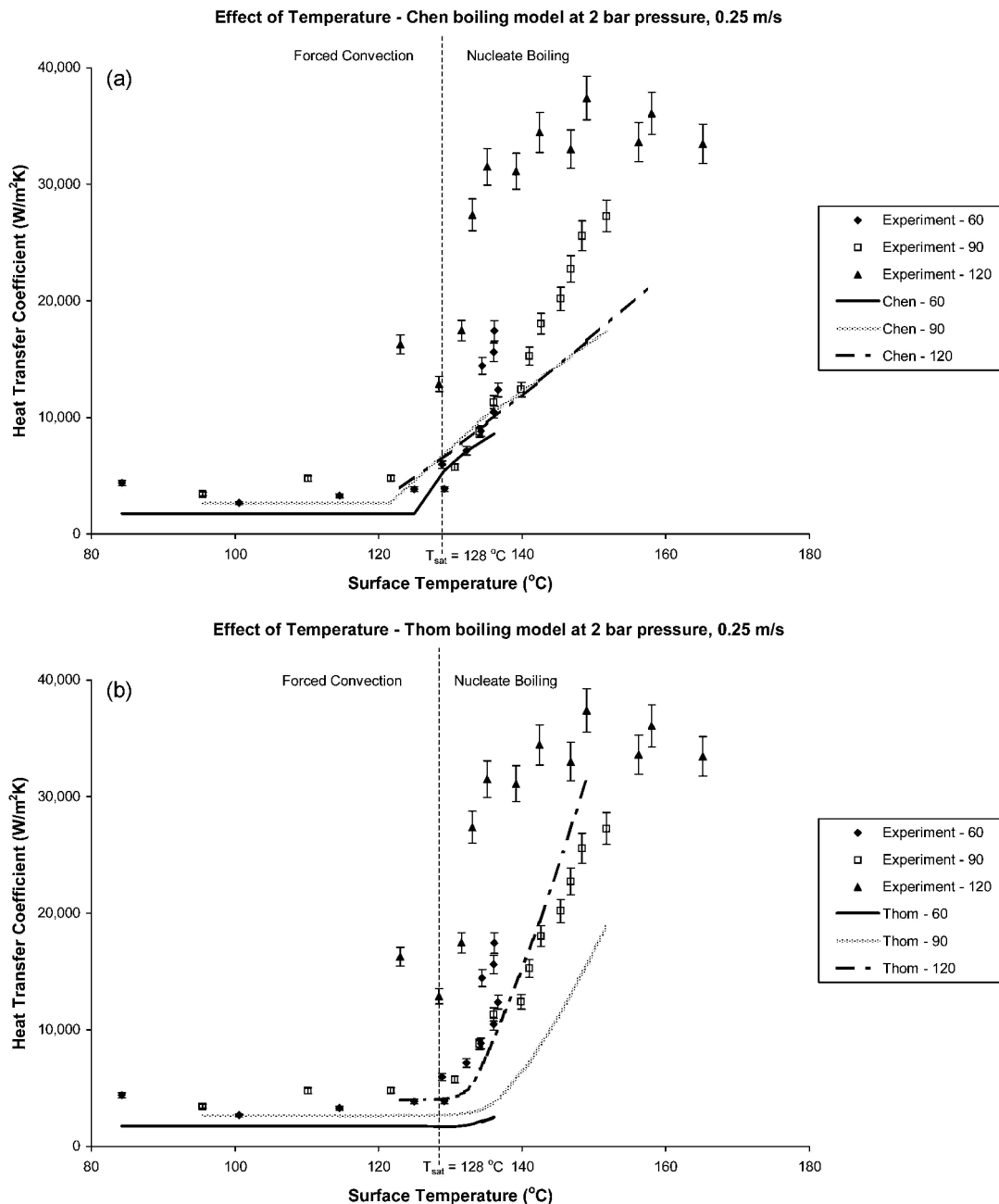


Fig. 8 (continued over)

a CFD modelling environment due to the difficulty in defining a characteristic length within the model and the number of fluid/vapour properties that are required.

The Cipolla model was found to have the largest mean error, 41.2 per cent, and often underpredicted measurements by a large amount. This model did represent the parametric trends in the experiments well, but the absolute values were often too low.

The Thom model followed the parametric variations well apart from pressure. It was found that, for most test conditions, this model gave the most accurate prediction of the experimental results. Models based on the partial boiling method are the most straightforward to

implement into a CFD environment. It is considered that this model should be used to study nucleate boiling heat transfer in IC engines.

ACKNOWLEDGEMENTS

The support of the EPSRC, Visteon, Ford Motor Company Limited and Ricardo Consulting Engineers throughout this work is gratefully acknowledged. Gratitude is also expressed to the Powertrain and Vehicle Research Unit at the University of Bath for supporting this work.

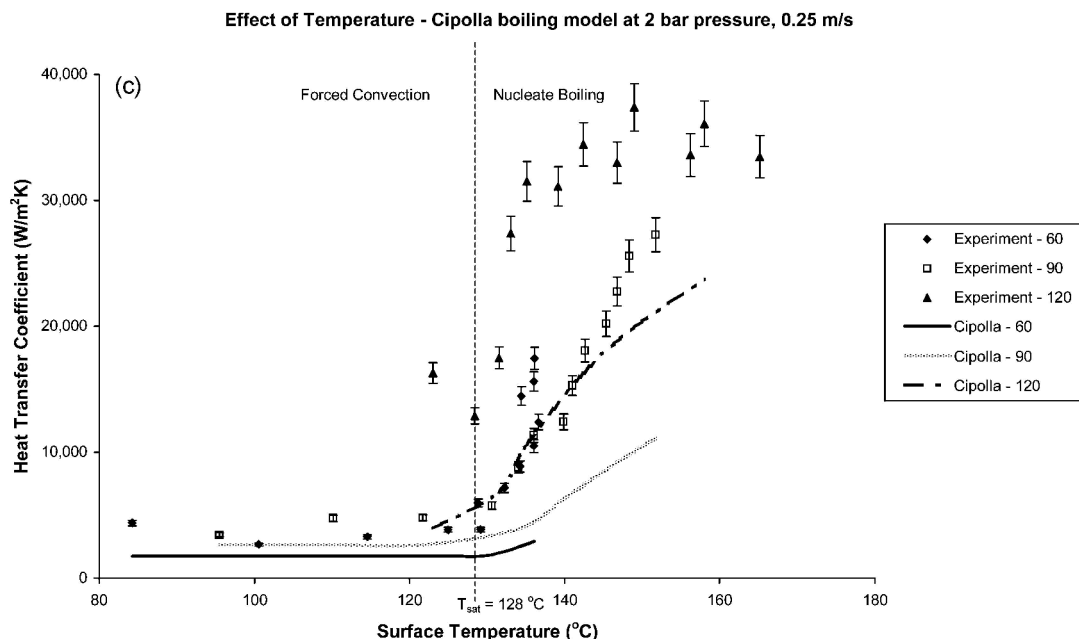


Fig. 8 Effect of fluid temperature: (a) Chen boiling model, (b) Thom boiling model and (c) Cipolla boiling model

Table 2 Overall mean deviation and mean deviation of models against experimental data

Velocity (m/s)	Pressure (bar)	Inlet temperature (°C)	Chen (%)	Thom (%)	Cipolla (%)
0.25	1	90	51.9	42.1	50.3
0.25	2	60	51.8	53.0	53.1
0.25	2	90	53.8	36.1	52.5
0.25	2	120	66.9	56.7	61.7
0.25	3	90	38.5	26.2	35.4
0.5	2	90	43.7	37.0	47.8
0.5	3	90	35.1	35.1	37.8
1	1	90	41.6	32.3	48.2
1	2	60	26.9	26.9	26.9
1	2	90	32.0	33.0	35.1
1	2	120	65.8	63.1	68.0
1	3	90	29.4	30.1	30.1
3	2	90	33.5	33.5	33.5
3	3	90	21.4	21.4	21.4
5	2	90	30.8	30.8	30.8
5	3	90	26.1	26.1	26.1
Overall mean deviation			40.6	36.4	41.2

REFERENCES

- 1 Kanefsky, P., Nelson, V. A. and Ranger, M. A systems engineering approach to engine cooling design. In SAE International Truck and Bus Meeting and Exposition, SP-1541, 1999-01-3780, Detroit, Michigan, 15–17 November, 1999.
- 2 Chen, J. C. Correlation for boiling heat transfer to saturated fluids in convective flow. *I&EC—Process Des. Develop.*, 1966, 5, 3.
- 3 Thom, J. R. S., Walker, W. M., Fallon, T. A. and Reising, G. F. S. Boiling in subcooled water during flow up heated tubes or annuli. *Proc. Instn Mech. Engrs*, 1965, 180(3C).

- 4 Cipolla, G. Heat transfer correlations applicable to the analysis of IC engine head cooling. In Proceedings of the International Centre for Mass and Heat Transfer conference, Dubrovnic, September 1987 (1989, Hemisphere, New York), pp. 373–396.
- 5 Robinson, K., Campbell, N. A. F., Hawley, J. G. and Leathard, M. J. Predicting heat transfer in simulated IC engine cooling galleries. In VTMS 6, IMechE/SAE, Brighton, 18–21 May 2003, Paper C599/038/2003, pp. 787–803.
- 6 Robinson, K. IC engine coolant heat transfer studies. PhD thesis, University of Bath, 2001.
- 7 Collier, J. G. and Thome, J. R. *Convective Boiling and Condensation*, 3rd edition, 1994 (Oxford University Press, Oxford).

- 8 **Robinson, K., Hawley, J. G., Hammond, G. P. and Owen, N. J.** Convective coolant heat transfer in internal combustion engines. *Proc. Instn Mech. Engrs, Part D: J. Automobile Engineering*, 2003, **217**(D2), 133–146.
- 9 **Kreith, F. and Bohn, M. S.** *Fundamentals of Heat Transfer*, 1986 (Harper and Row, New York).
- 10 **Gollin, M., McAssey, E. V. and Stinson, C.** Comparative performance of ethylene glycol/water and propylene glycol/water coolants in convective and forced flow boiling regimes. SAE paper 950464, 1995.
- 11 **Davis, E. J. and Anderson, G. H.** The incipience of nucleate boiling in forced convection flow. *Am. Inst. Chem. Engrs J.*, 1966, **12**(4), 774–780.
- 12 **Bergles, A. E. and Rohsenow, W. M.** The determination of forced convection surface boiling heat transfer. ASME paper 63, HT-22, 1963.
- 13 **Bjorge, R. W., Hall, G. R. and Rohsenow, W. M.** Correlation of forced convection boiling heat transfer data. *Int. J. Heat Mass Transfer*, July 1982, **25**, 753.
- 14 **Son, G., Dhir, V. K. and Ramanujapu, N.** Dynamics and heat transfer associated with a single bubble during nucleate boiling on a horizontal surface. *Trans. ASME, J. Heat Transfer*, 1999, **121**(3), 623–631.
- 15 **Versteeg, H. K. and Malalasekera, W.** *An Introduction to Computational Fluid Dynamics—The Finite Volume Method*, 1995 (Longman, London).
- 16 **Leathard, M. J.** Computational modelling of coolant heat transfer in internal combustion engines. PhD thesis, University of Bath, 2002.
- 17 **Wambsganss, W. M., France, D. M., Jendrzeczyk, J. A. and Tran, T. N.** Boiling heat transfer in a horizontal small-diameter tube. *Trans. ASME, J. Heat Transfer*, 1993, **115**, 963–972.
- 18 **Campbell, N. A. F.** The influence of nucleate boiling in engine cooling and temperature control. PhD thesis, University of Bath, 2001.

Copyright of Proceedings of the Institution of Mechanical Engineers -- Part D -- Journal of Automobile Engineering is the property of Professional Engineering Publishing and its content may not be copied or emailed to multiple sites or posted to a listserv without the copyright holder's express written permission. However, users may print, download, or email articles for individual use.